Biochemical Pharmacology 79 (2010) 1418–1427

Contents lists available at ScienceDirect

Biochemical Pharmacology

journal homepage: www.elsevier.com/locate/biochempharm

Differential inhibition of restriction enzyme cleavage by chromophore-modified analogues of the antitumour antibiotics mithramycin and chromomycin reveals structure–activity relationships

Sylvia Mansilla [a], Irene Garcia-Ferrer [a], Carmen Méndez [b], José A. Salas [b], José Portugal [a,*]

[a] Instituto de Biologia Molecular de Barcelona, CSIC, Parc Cientific de Barcelona, Baldiri Reixac, 10, E-08028 Barcelona, Spain
[b] Departamento de Biologia Funcional-Instituto Universitario de Oncologia del Principado de Asturias, Universidad de Oviedo, E-33006 Oviedo, Spain

ARTICLE INFO

Article history:
Received 12 November 2009
Accepted 11 January 2010

Keywords:
Mithramycin A
Chromomycin A_3
Restriction enzymes
Antitumour antibiotics
Carcinoma cells

ABSTRACT

Differential cleavage at three restriction enzyme sites was used to determine the specific binding to DNA of the antitumour antibiotics mithramycin A (MTA), chromomycin A_3 (CRO) and six chromophore-modified analogues bearing shorter side chains attached at C-3, instead of the pentyl chain. All these antibiotics were obtained through combinatorial biosynthesis in the producer organisms. MTA, CRO and their six analogues showed differences in their capacity for inhibiting the rate of cleavage by restriction enzymes that recognize C/G-rich tracts. Changes in DNA melting temperature produced by these molecules were also analyzed, as well as their antiproliferative activities against a panel of colon, ovarian and prostate human carcinoma cell lines. Moreover, the cellular uptake of several analogues was examined to identify whether intracellular retention was related to cytotoxicity. These experimental approaches provided mutually consistent evidence of a seeming correlation between the strength of binding to DNA and the antiproliferative activity of the chromophore-modified molecules. Four of the analogues (mithramycin SK, mithramycin SDK, chromomycin SK and chromomycin SDK) showed promising biological profiles.

1. Introduction

Mithramycin A (MTA) and chromomycin A_3 (CRO) are members of the aureolic acid family of anticancer antibiotics. MTA is produced by *Streptomyces argillaceus* (ATCC 12596), among other species, while CRO is produced by *Streptomyces griseus* subsp. *griseus* (ATCC 31053) [1]. These antibiotics are glycosylated aromatic polyketides, in which two different oligosaccharide chains are attached in the aromatic polyketide moiety (Fig. 1) [1,2].

MTA has been used in the treatment of Paget's disease and advanced testicular carcinoma [3], while CRO has been used in Japan against advanced stomach cancers [4]. The aureolic acid family of molecules has gained renewed attention as therapeutic agents in both cancer and non-cancer related diseases [5–8]. MTA has been proposed for the treatment during antiangiogenic strategies against pancreatic cancer [9]. The activity of these antibiotics has been associated with their ability to bind to G/C-rich DNA tracts via the minor groove [10–14], and divalent cations such as Mg^{2+} are essential requirement for the association with DNA at and above physiological pH [15,16]. As a consequence of the binding to DNA these antibiotics are able to inhibit transcription both *in vivo* and *in vitro* [17–20]. Sequence-selective binding of MTA and CRO to DNA is fundamentally achieved through direct hydrogen bonding between the 8-O-hydroxyl group in the antibiotic molecules and the 2-amino group of the guanine at GpC or GpG steps, while their respective trisaccharide moieties are essential for optimal binding [13,14,21,22]. The thermodynamic analysis of the MTA and CRO binding to DNA has shown that this is entropically driven [16,23], dominated by the hydrophobic transfer of the Mg^{2+}-coordinated antibiotic dimers from solution to the DNA-binding site [23]. Hydrogen bonding also participates in the binding of the oligosaccharide chains along the minor groove [13,21,22,24].

Despite the high structural similarity between MTA and CRO (Fig. 1), the genetic organization of the biosynthesis gene clusters for both antitumour antibiotics is highly different [25]. These gene clusters have been studied in detail by gene sequencing, insertional inactivation and gene expression [1,11,25–29]. In fact, most of the biosynthetic intermediates in these pathways have been isolated and characterized, and some of them have shown enhanced antitumour activity [17,18,20,29].

Since MTA and CRO exhibit severe side-effects, we examined the possibility that some biosynthetically produced analogues (Fig. 1) may present lower toxicity and higher antitumour activity.

* Corresponding author. Tel.: +34 93 403 4959; fax: +34 93 403 4979.
E-mail address: jpmbmc@ibmb.csic.es (J. Portugal).

0006-2952/$ – see front matter © 2010 Elsevier Inc. All rights reserved.
doi:10.1016/j.bcp.2010.01.005

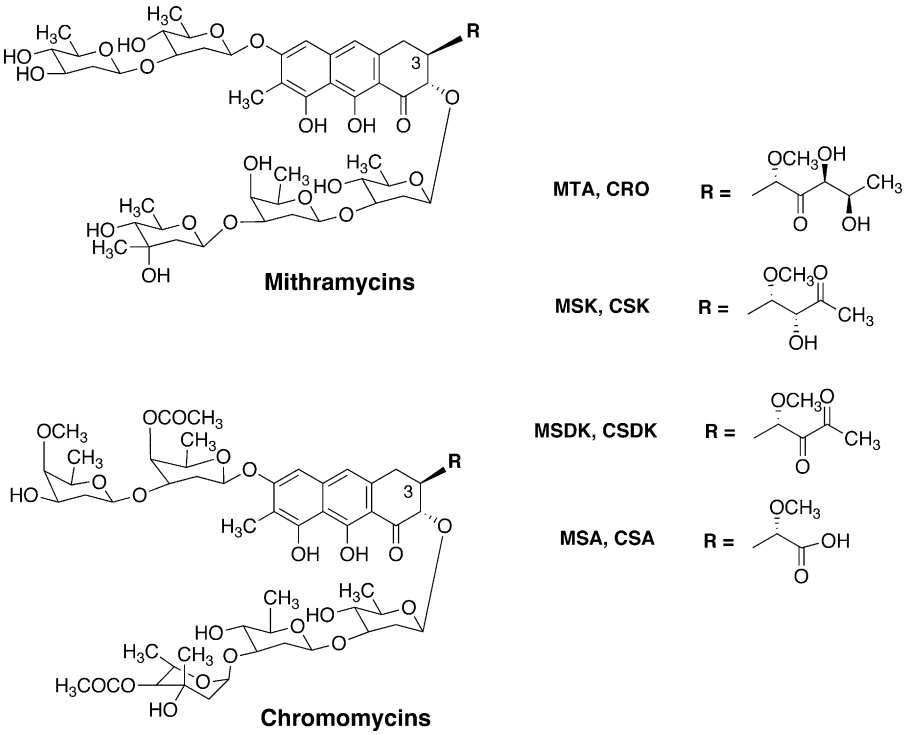

Fig. 1. Chemical formulae of mithramycins and chromomycins. Mithramycin A (MTA), mithramycin SK (MSK), mithramycin SDK (MSDK), mithramycin SA (MSA), chromomycin A_3 (CRO), chromomycin SK (CSK), chromomycin SDK (CSDK) and chromomycin SA (CSA).

Therefore, we analyzed whether six biosynthetically produced molecules related to MTA and CRO, which exhibit an array of structural changes in the highly functionalized pentyl side chain attached at three-position in MTA and CRO (Fig. 1), displayed differences in sequence-selective binding to C/G-rich regions in DNA that might be correlated to dissimilar cytotoxic activity. We have explored whether the information provided by differential restriction enzyme cleavage in the presence of MTA, CRO or any of the six chromophore-modified molecules may give insights into structure–activity relationship among the different aureolic acid antibiotics, and whether these studies might unveil any superior antiproliferative activity among the chromophore-modified molecules.

Our results were consistent with that the analysis of the inhibition of restriction enzyme cleavage by small drugs is a useful approach to determine DNA-binding preferences [30,31]. Besides, a clear correlation was observed between the capacity for inhibiting restriction enzyme cleavage by the different molecules and the increase in DNA melting temperature. We also acquired information on the antiproliferative activity of the different mithramycins and chromomycins by using a variety of human carcinoma cell lines. Moreover, because intracellular drug retention might be related to cytotoxicity, we examined the cellular uptake of a selected set of those antibiotics using two different human carcinoma cell lines. Altogether, these experimental approaches provided mutually consistent evidence of a seeming correlation between the strength of binding to DNA and the biological activity of the chromophore-modified aureolic acid antibiotics.

2. Materials and methods

2.1. Mithramycins, chromomycins, DNA substrates and restriction enzymes

Mithramycin A (MTA), mithramycin SK (MSK), mithramycin SDK (MSDK), mithramycin SA (MSA), chromomycin A_3 (CRO), chromomycin SK (CSK), chromomycin SDK (CSDK), and chromomycin SA (CSA) (Fig. 1) were isolated and purified from the producing organisms as described previously [11,25], and their purity (≥95%) was checked by HPLC. Samples of the different antibiotics were prepared as 1 mM or 500 μM solutions in 80 mM NaCl, 20 mM Hepes (pH 7.5), and kept at −20 °C. Fresh diluted solutions were prepared using the appropriate restriction enzyme buffer, see below, which contained Mg^{2+} ions required to dimerize the different aureolic acid antibiotics.

Plasmid pBR322 was purified from transformed *E. coli* HB101 using the Qiagen Plasmid Maxi Kit (Servicios Hospitalarios, Barcelona, Spain), and linearized by cleavage with *BamHI*. The complete linearization was verified by agarose gel electrophoresis. *Eco52I* (*EagI*), *Bsp68I* (*NruI*) and *AatII*, purchased from Fermentas (Quimigen, Madrid, Spain), were used for restriction enzyme assays using the buffers recommended by the vendor: 100 mM NaCl, 3 mM $MgCl_2$, 10 mM Tris–HCl (pH 8.5) and 0.1 mg/ml BSA (*Eco 52I*), 100 mM NaCl, 10 mM $MgCl_2$, 50 mM Tris–HCl (pH 7.5) and 0.1 mg/ml BSA (*Bsp68I*) and 66 mM K–acetate, 10 mM Mg–acetate, 30 mM Tris–acetate (pH 7.9) and 0.1 mg/ml BSA (*AatII*). All these enzymes cleave the pBR322 plasmid DNA at unique sites (Fig. 2A).

DNA from salmon testes (Sigma, St. Louis, MO) was dissolved in 80 mM NaCl, 20 mM Hepes (pH 7.5), sonicated, phenol extracted twice and dialyzed against the same buffer.

2.2. Analysis of the effects of mithramycins and chromomycins on the rate of cleavage of pBR322 plasmid DNA by restriction enzymes

The effects of the different analogues on the first-order rate constant at the individual restriction enzyme sites were determined as described elsewhere [31]. In brief, all DNA–drug incubations and the time-course digestions with restriction enzymes were carried out in the buffers stated above which contained enough $MgCl_2$ to assure the Mg^{2+}-mediated dimerization of mithramycins and

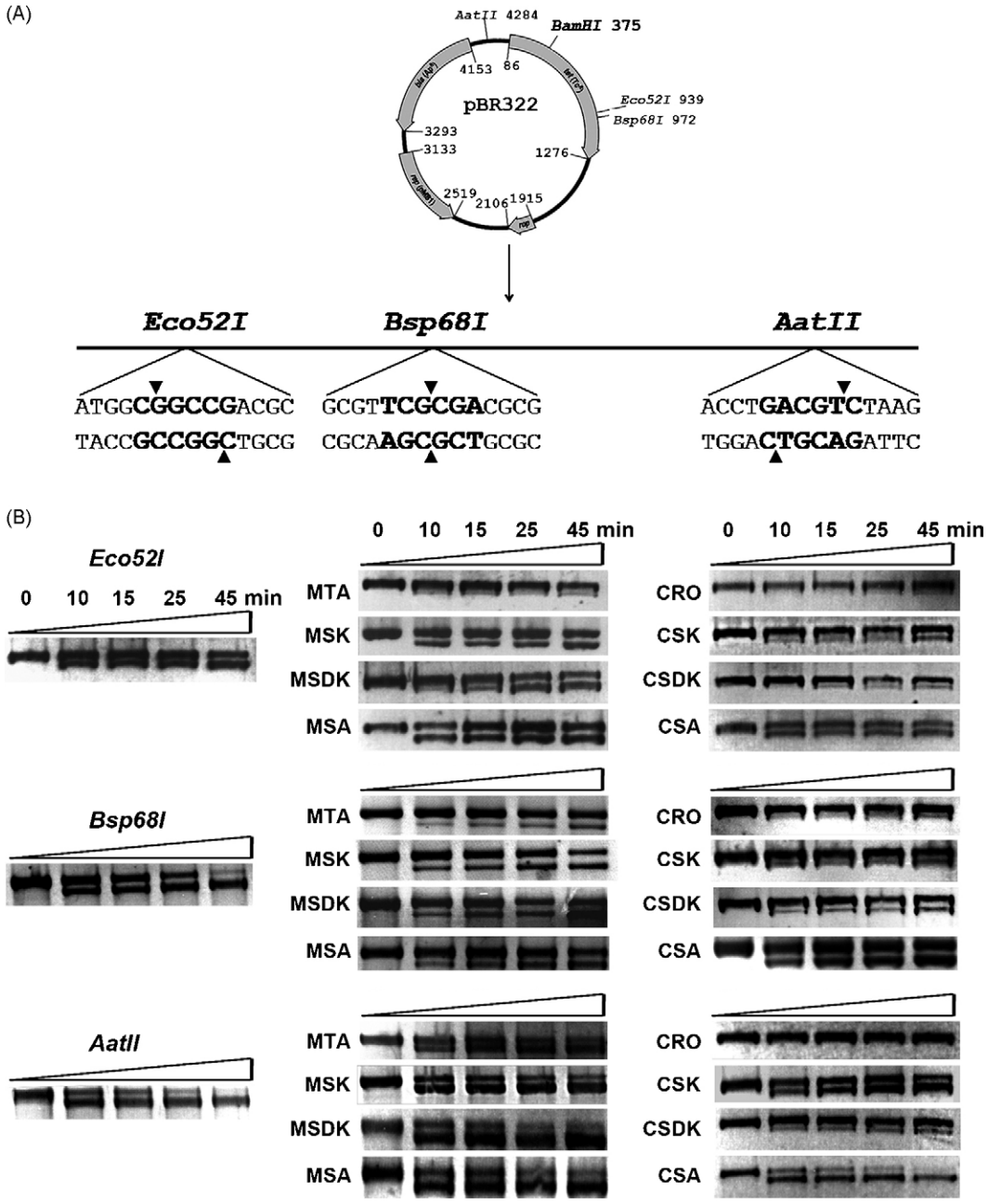

Fig. 2. Inhibition of restriction enzyme cleavage. (A) Map of the pBR322 plasmid showing the sequences surrounding the *Eco52I* (*EagI*), *Bsp68I* (*NruI*) and *AatII* sites. (B) Representative agarose gels depicting the time-course of cleavage of linearized pBR322 by *Eco52I*, *Bsp68I* or *AatII* restriction enzymes in the absence (left panels) or the presence of the different aureolic acid antibiotics. In the experiment depicted in the figure, the drug/DNA (bp) molar ratio was 0.2, which corresponds to a stoichiometry of 5 mol of bp per 1 mol of either MTA, MSK, MSDK or MSA, and to a drug/DNA (bp) molar ratio of 0.15, which corresponds to about 6.7 mol of bp per 1 mol of antibiotic in the experiments with CRO, CSK, CSDK or CSA.

chromomycins [15,16]. DNA cleavage reactions containing 40 μM (in bp) DNA and either 6 μM or 8 μM drug (corresponding to drug/DNA ratios of 0.15 and 0.20, respectively) were pre-incubated at 25 °C for 20 min, and the cleavage reactions initiated at 37 °C by the addition of the appropriate enzyme. At known time intervals, aliquots were removed from the reaction tube and the digestions were stopped by adding 5% glycerol in 10 mM EDTA (pH 7.0), containing 0.04% Orange G (Sigma), followed by the inactivation of the enzyme at 65 °C for 5 min. The digestion products were resolved by electrophoresis on 1.2% agarose gels in Tris/Borate/EDTA buffer, run at 10 V/cm. Gel tracks were loaded with about 0.1 μg DNA. After running, the gels were stained with ethidium bromide, documented using a GeneGenius BioImaging system (Syngene, Cambridge, UK) and quantified using the GeneTools 3.07 software (Syngene). Linear least-squares fit of the logarithm of the relative amount of uncut DNA *versus* time renders the first-order rate constant for cleavage at each restriction site [30].

2.3. Thermal denaturation studies

Ultraviolet DNA melting curves in the presence of eight different mithramycins and chromomycins were determined using a Jasco VP-650 spectrophotometer (Jasco Analitica, Madrid, Spain) equipped with a Jasco ETC-717 temperature controller that was programmed to heat the samples from 30 to 100 °C at 1 °C/min, taking absorbance readings at 260 nm every 20 s. Solutions of sonicated salmon testes DNA in 80 mM NaCl, 1 mM $MgCl_2$, 20 mM Hepes (pH 7.5) [final concentration 20 μM (bp)] containing any of

the aureolic acid antibiotic at known molar ratios were prepared by direct mixing with aliquots from stock solutions of the drugs, followed by incubation at 30 °C for 30 min prior to the DNA melting analysis. *Tm* values were calculated from absorbance *versus* temperature melting curves by standard procedures used to evaluate drug–DNA interactions [32].

2.4. Cell culture and antiproliferative assays

The human cancer cell lines IGROV-1 (ovarian), OVCAR-5 (ovarian), PC-3 (prostate) and DU-145 (prostate) were maintained in DMEM (Invitrogen, Prat de Llobregat, Spain). HT-29 (colon) was cultured in RPMI (Invitrogen) and HCT116 (colon) in 50% DMEM (Invitrogen)/50% Ham's F-12 medium (Lonza, Barcelona, Spain). All the cell cultures were supplemented with 10% fetal bovine serum (Invitrogen), 100 units/ml penicillin, and 100 μg/ml streptomycin. Cells were grown at 37 °C under a humidified atmosphere containing 5% CO_2.

For the antiproliferative assays, cells were plated in 96-well plates (Corning Costar, Cultek, Madrid, Spain) at a density of 1×10^4 cells/well, 24 h prior to addition of the tested drug. After 72 h of incubation, the different mithramycins and chromomycins were removed and the cells were washed. The antiproliferative activity was measured by the MTT-assay [33] using 3-(4,5-

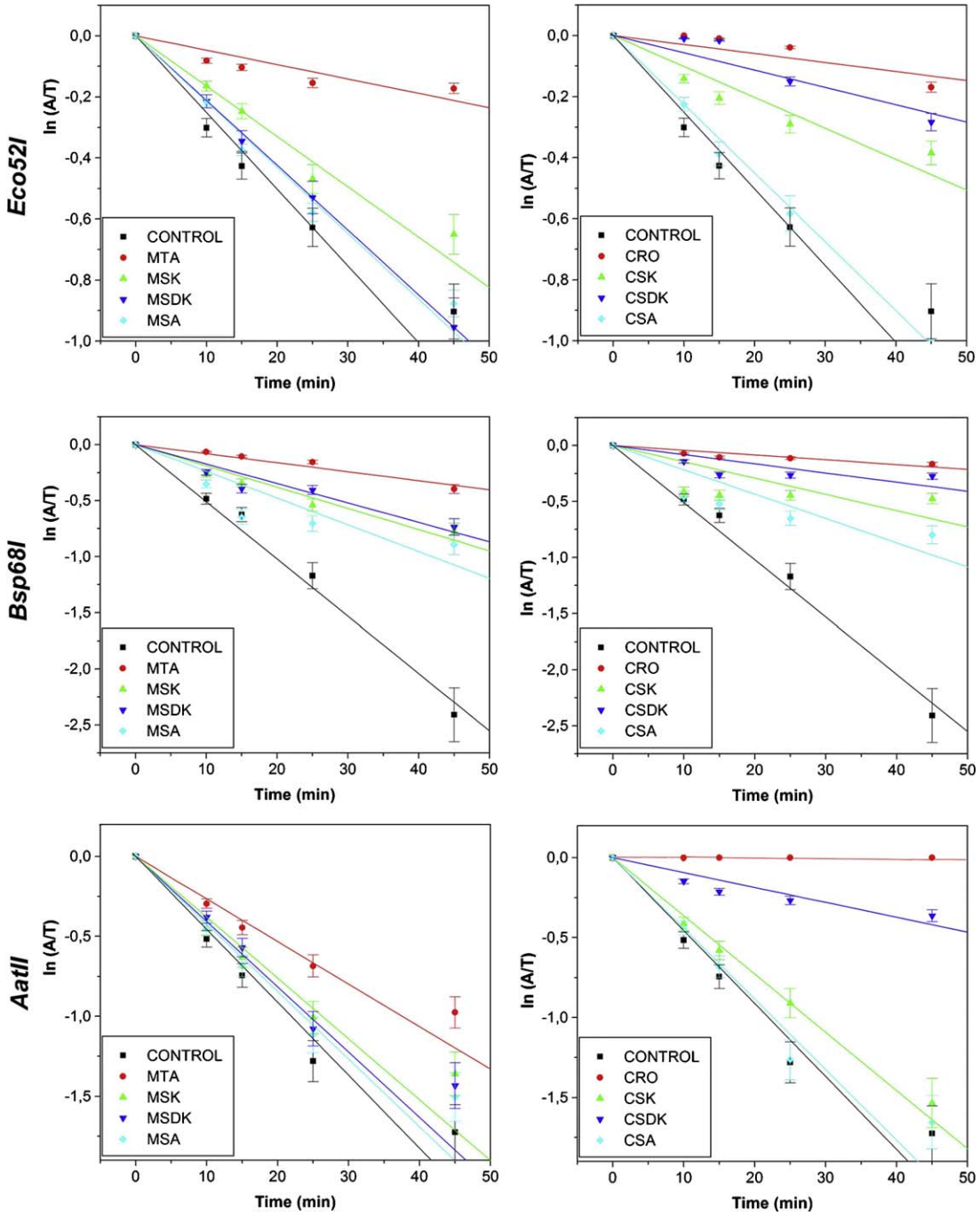

Fig. 3. Rates of cleavage of the *Eco52I*, *Bsp68I* and *AatII* at the unique restriction sites in pBR322 DNA. The different panels present data (mean ± SD) from three independent experiments in either absence or presence of MTA, MSK, MSDK, MSA, CRO, CSK, CSDK or CSA. The plots display the uncleaved fraction, in a logarithmic scale, in which *A* is the uncleaved DNA, and *T* is the total DNA, quantified from agarose gels as a function of time. First-order rate constants were calculated from the slopes of the least-squares fit of the experimental data.

dimethylthiazolyl)-2,5-diphenyltetrazolium bromide (Sigma). For the easy of plotting and comparison, values are presented as $-\log(IC_{50})$, where IC_{50} is the drug concentration (Molar) that reduced cell proliferation by 50%.

2.5. Flow cytometric monitoring of mithramycins and chromomycins in HCT116 and PC-3 cells

The uptake and retention of the different aureolic acid antibiotics by HCT116 and PC-3 human carcinoma cells was analyzed with a Coulter Epics-XL flow cytometer (Coulter Corporation, Hialeah, FL). Cells cultured to a final density of 2.5×10^4 cells/ml were incubated with a 150 nM solution of each antibiotic for different periods of time ranging from 4 to 72 h. Cells were then collected, washed with ice-cold PBS, and propidium iodide was added up to 20 μg/ml to measure the number of viable cells after treatment. The intracellular fluorescence produced by the uptake of the different drugs was measured by setting the flow cytometer to λ_{ex} 470 nm and λ_{em} 550 nm. Mean fluorescence values were acquired from 1000 viable, propidium iodide-negative, cells gated for analysis. All experiments were repeated twice to confirm reproducibility (±5%).

3. Results

We analyzed the differential cleavage by *Eco52I* (*EagI*), *Bsp68I* (*NruI*) and *AatII* restriction enzymes, which recognize and cut unique C + G-rich target sites in the pBR322 plasmid (Fig. 2A), in the presence/absence of eight aureolic acid antibiotics, which chemical structures are displayed in Fig. 1. Digestion of *BamHI*-linearized pBR322 by any of these enzymes resulted in the initial appearance of three electrophoretic bands on an agarose gel. They corresponded to the undigested pBR322 and two fragments that were the products of the enzyme cleavage at their unique site within this DNA. All the digestions were carried out with each restriction enzyme under experimental conditions in which the reactions follow a first-order kinetics. Fig. 2B shows representative examples of experiments undertaken in triplicate (note that the smaller fragment has migrated too far to be seen). The different panels depict the time-course of digestion of the linearized pBR322 DNA in the absence and presence of the different mithramycins and chromomycins. All the restriction cleavage experiments were done at mole ratios corresponding to the 1:5 (drug/DNA (bp)) stoichiometry, although other drug/DNA molar ratios were also studied (see legend to Fig. 2B). The binding stoichiometry of several of aureolic acid antibiotics to DNA was determined previously to be 4–5 mol of bp per mol of drug [15,16,23].

Based on the quantification of the electrophoretic bands shown in Fig. 2B, Fig. 3 shows plots of the ratio between the amount of uncleaved band and the total of DNA (in a logarithm scale) *versus* digestion time. The slopes for these plots were used to calculate the first-order rate constants in the absence, or in the presence, of the different antibiotics [30,31,34]. For the sake of comparison, Fig. 4 shows histograms of the ratio between the cleavage rate constants in the presence of each drug (k) and the rate of cleavage in their absence (ko). This figure illustrates the relative "effectiveness" of every mithramycin (Fig. 4A), or chromomycin (Fig. 4B), to reduce the rate of DNA cleavage by each restriction enzyme. For all these antibiotics, inhibition was higher for *Bsp68I* (5′-TCGCGA-3′) than for either *Eco52I* (5′-CGGCCG-3′) or *AatII* (5′-GACGTC-3′). *Bsp68I* and *Eco52I* cleave sequences that contain the GpC step, which is considered the preferred binding site for MTA and CRO within a zone of three/four contiguous cytosines or guanines [12–14,22,35]. *AatII*, which recognizes and cuts a restriction site containing an isolated CpG site, was less protected by any mithramycin (Fig. 4), although it was strongly protected by CRO, a peculiarity that will be discussed below.

In general, the results obtained in the restriction enzyme experiments were consistent with that all mithramycins and chromomycins bind preferentially to DNA regions containing, at least, two contiguous cytosine and/or guanines, as it has been observed for MTA and CRO by using several techniques [10,12–14,22]. However, some binding to isolated CpG steps (as in *AatII* restriction site) is required to explain the degree of inhibition observed with the different molecules (Figs. 3 and 4). Protection of some isolated C/G zones has been reported in footprinting studies [35].

When *Eco52I* was used, the protection from cleavage followed the order MTA > MSK > MSDK > MSA. However, for *Bsp68I* and *AatII* this was slightly different, MTA > MSDK ≥ MSK > MSA. These results indicate that MTA and MSDK may be more tolerant to alternate cytosines and guanines other than the 'preferred' GpC step. Overall, the inhibition of restriction cleavage was higher for CRO and their analogues compared to mithramycins (Figs. 3 and 4); the exception was CSA, which protection of the three restriction sites was closer to that of MSA (cf. Fig. 4A and B). When *Eco52I* or *Bsp68I* restriction enzymes were used, the protection from cleavage by chromomycins followed the order CRO > CSDK > CSK > CSA. Furthermore, both CRO and CSDK protected DNA from *AatII* cleavage very efficiently compared to the effect of the other chromomycins (Fig. 4B) and to their analogues MTA or MSDK. These results indicate that CRO and CSDK may be more tolerant to the presence of CpG steps within their binding sites, as already occurred for MTA. For the four chromomycins, the sequence CGCG, which is found within the *Bsp68I* recognition site (Fig. 2A), appeared to be the best-protected sequence as indicated

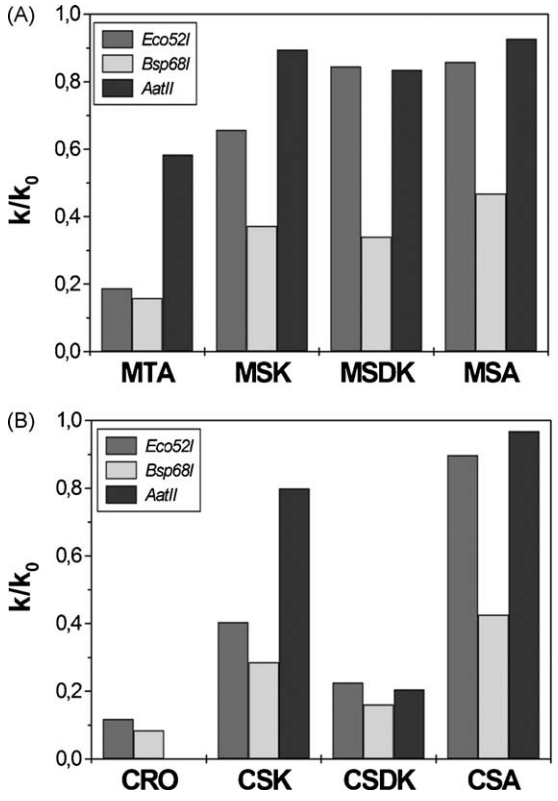

Fig. 4. Comparison of the relative rate of cleavage of linearized pBR322 DNA by *Eco52I*, *Bsp68I* or *AatII*. The histograms show the change in the rate of restriction cleavage as the ratio between the restriction enzyme cleavage in the presence of the different mithramycins and chromomycins (k) and in their absence (ko). Lower values represent, therefore, a higher degree of inhibition (see also Table 1).

Table 1
Effects of mithramycins and chromomycins on DNA melting temperature, the cleavage of linearized pBR322 plasmid by *Bsp68I*, and on the proliferation of human carcinoma cell lines.

	Tm (°C)	Δ*Tm* (°C)	Protection of 5′-TCGCGA-3′ (%)[a]	Antiproliferative activity[b]
Salmon testes DNA	81.6	–	–	–
Mithramycin A	86.5	4.9	84.2	7.08 ± 0.42 (6)
Mithramycin SK	83.6	2.0	62.8	7.40 ± 0.31 (6)
Mithramycin SDK	84.3	2.7	66.0	7.96 ± 0.49 (6)
Mithramycin SA	82.0	0.4	53.2	6.11 ± 0.29 (4)
Chromomycin A_3	86.8	5.2	91.6	8.14 ± 0.45 (6)
Chromomycin SK	85.2	3.6	71.5	7.52 ± 0.42 (3)
Chromomycin SDK	85.7	4.1	83.9	7.82 ± 0.13 (3)
Chromomycin SA	82.4	0.8	57.4	7.51 ± 0.34 (3)

[a] Percentage of protection from restriction cleavage by *Bsp68I* = $(1-(k/ko))\times 100$. The *k*/*ko* values are shown in Fig. 4.
[b] Antiproliferative activities determined for a variety of human carcinoma cell lines. Data are shown as $-\log(IC_{50})$—in which IC_{50} is the drug concentration (Molar) that inhibits cell proliferation by 50%. Data (mean ± SD) correspond to the experimental values obtained for the panel of cell lines shown in Fig. 5.

by the lower *k*/*ko* ratio values (Fig. 3). Moreover, as mentioned above, CRO protected the *AatII* site from cleavage very efficiently (Figs. 3 and 4B), which may indicate a higher tolerance of CRO to the presence of isolated CpG sites, compared to MTA and the chromophore-modified derivatives. Besides, CSDK was better than MSDK at protecting from any restriction enzyme cleavage, and the inhibition reached values closed to that obtained with CRO. Why CRO had such strong inhibiting effect on *AatII* cleavage, even though the 'preferred' GpC or GpG steps [13,22] are absent, remains unidentified, although it might be tentatively explained by the presence of other cytosines and guanines flanking the restriction site, which can encompass, for example, a potential ACCTG binding site at the 5′-edge of the restriction site (Fig. 2A). In this respect, the presence of an acetoxy group in the sugars of the chromomycins has been suggested to impart some distinctive features to its binding to DNA [36]. It has been shown by DNAse I footprinting that MTA protects the TCGCGA sequence (*Bsp68I* restriction site) from DNAse I cleavage better than CGGCCG (*Eco52I* restriction site) [35], in line with the relative degree of protection observed in the restriction cleavage assays (Fig. 4). The stronger inhibition by *Bsp68I* reaction by the aureolic acid antibiotics compared to the other restriction enzymes (Fig. 4) was consistent with the preferential interaction of the drugs at or near the restriction site. The optimal cleavage conditions for the restriction enzyme reactions included the use of buffers of different ionic strength, Mg^{2+} concentration, and pH—see the composition of the digestion buffers in Section 2.1. Nevertheless, *Bsp68I* cleavage was inhibited strongly by the different drugs regardless of the higher salt content of its buffer, which suggests that the composition of the different buffers had little effect of the binding of the antibiotics to DNA. These results were consistent with our previous observation that changes in the concentration of monovalent cations have little consequences on MTA binding, while Mg^{2+} is an essential requirement for binding to DNA [23].

We have also examined the effects of the eight aureolic acid antibiotics (Fig. 1) on the DNA melting temperatures as an indication of their potential to interact with heterogeneous DNA [32]. The complete set of UV DNA melting experiments undertaken at different drug/DNA molar ratios is shown online as Supplementary Fig. S1. The increase in DNA melting temperatures induced by these antibiotics (Δ*Tm*) is shown in Table 1 alongside with the quantification of the percentage of protection at, or near the, *Bsp68I* restriction site. The *Tm* values summarized in Table 1 correspond to experiments performed in the presence of 7 μM drug (drug/DNA (bp) molar ratio of 0.35, which corresponds to about one mole of antibiotic per 3 mol of bp, enough to saturate the polynucleotide lattice [23]). We did not intend, at this point, to obtain a quantitative measurement of binding parameters for each analogue, such as their apparent binding constants, but a rough estimation of their relative strength of binding to DNA. MTA and CRO produced the higher increase in the melting temperatures, while MSA and CSA had the smaller effect among all the molecules. According to the results shown in Table 1, a rough estimate of the strength of binding to DNA would be: CRO > MTA > CSDK > CSK > MSDK > MSK > CSA > MSA. In any case, the relative capacity of those molecules to increase the DNA melting temperature was in keeping with the binding affinities determined previously for MTA, MSK and CRO [15,16,23]. In addition, CRO strongly protected DNA from cleavage regardless of the enzyme used, and it caused the higher increase in DNA melting. The linear correlation between the Δ*Tm* values and the percentages of inhibition of cleavage by *Bsp68I* was rather good ($r = 0.975$) (Table 1). Consequently, a hierarchical classification the aureolic acid antibiotics based on the changes produced in DNA melting temperature (Δ*Tm*) was fully consistent with their relative inhibition of restriction enzyme cleavage.

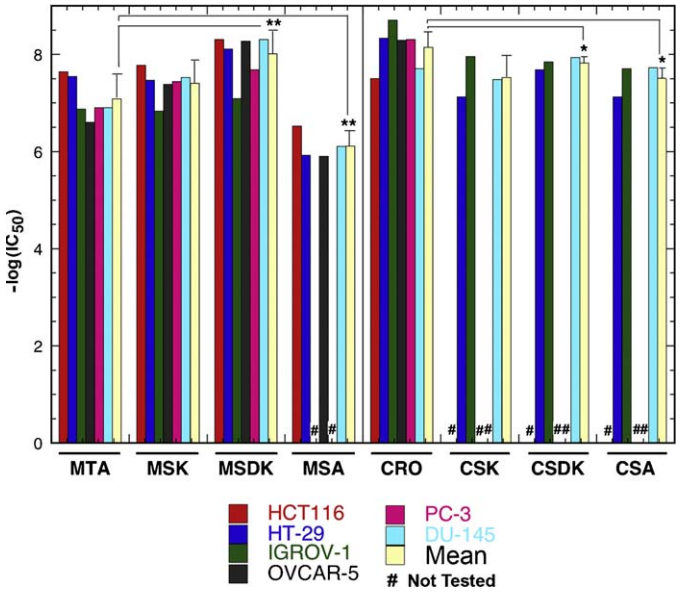

Fig. 5. Antiproliferative effects of mithramycins and chromomycins on human carcinoma cell lines. Colon carcinoma cell lines (HCT116, HT-29), ovarian carcinoma cell lines (IGROV-1, OVCAR-5) and prostate carcinoma cell lines (PC-3, DU-145) were used in the experiments. The presence of metabolically active cells was determined by the MTT-assay after 72-h continuous treatment with the drugs (data are average values from two independent experiments). For the sake of comparison, the figure also shows the average antiproliferative activities (mean ± SD) against the different types of carcinoma. Statistically significant differences in the antiproliferative activity of MTA or CRO compared to their respective analogues are indicated ($^{*}p < 0.05$, $^{**}p < 0.01$, unpaired Student's *t*-test for 3–6 independent experiments performed in duplicate).

Fig. 5 shows a comparison of the antiproliferative effects of the aureolic acid antibiotics on six human cells lines, which encompass colon, ovarian and prostate carcinomas. Data are presented as $-\log(IC_{50})$, the drug concentration that inhibits cell growth by a 50% in MTT-assays (see Section 2). For every molecule, Table 1 shows the $-\log(IC_{50})$ mean values (±SD) corresponding to the antiproliferative activity determined for each cell type from the experimental data shown in Fig. 5. The comparison of the antiproliferative response to the different mithramycins (Fig. 5 and Table 1) revealed that MSDK was the most active molecule followed by MSK and MTA, while MSA was less active. However, these average values might conceal some information that is only revealed through the scrutinization of the cytostatic/cytotoxic effects on every cell line (Fig. 5). For example, in HCT116 colon cells MSK and MSDK were the most active among the mithramycins, while MSDK was especially active against ovarian cells, in agreement with previous observations [11,17,18]. MSA showed a relatively low binding to DNA and the poorest antiproliferative activity. It seems that the shorter alkyl chain and the presence of a terminal acidic group in this chromophore-modified molecule (Fig. 1) may produce those results. The mean antiproliferative activity of chromomycins against a variety of human carcinoma cell lines showed that the three chromophore-modified molecules were biologically active (Fig. 5). However, their antiproliferative activities were lower than those for CRO. Nevertheless, when compared with mithramycins the three molecules showed similar activity (Fig. 5). Actually, CSA may possess stronger antiproliferative activity than MSA.

We examined whether the patterns of protection against restriction enzymes, and thus preferential DNA-binding sequences, as well as the increase in DNA melting temperatures, may correlate with the antiproliferative activity of chromomycins and mithramycins. Fig. 6 displays the linear regression calculated between the effects of the different molecules on the *Bsp68I* restriction site and the $-\log(IC_{50})$ values. The correlation observed ($r = 0.741$, $p < 0.05$) was fairly good. Furthermore, about 55% of the variance in the antiproliferative activity might be "explained" by the strength of binding to DNA (since $r^2 = 0.549$). In the correlation analysis only MTA and MSDK showed average values outside the 95% interval of confidence (Fig. 6). This behaviour would indicate that correlations between antiproliferative activity and DNA-binding are weaker among the mithramycin analogues. Tentatively, for MSDK this would mean it has an outstanding biological activity, which might only be partially explained by its DNA-binding preferences. CRO appeared to bind DNA tightly than its chromophore-modified analogues (Fig. 4B and Table 1) and it seems to be more cytotoxic/cytostatic, while CSDK showed higher antiproliferative activity than CSK and CSA. The evaluation of the different chromomycins using restriction enzyme cleavage (Figs. 2–4) and of their effect on DNA melting temperature (Fig. S1 and Table 1) indicated that the strength of binding of CRO or CSDK to DNA and their antiproliferative activity were clearly associated (Fig. 6).

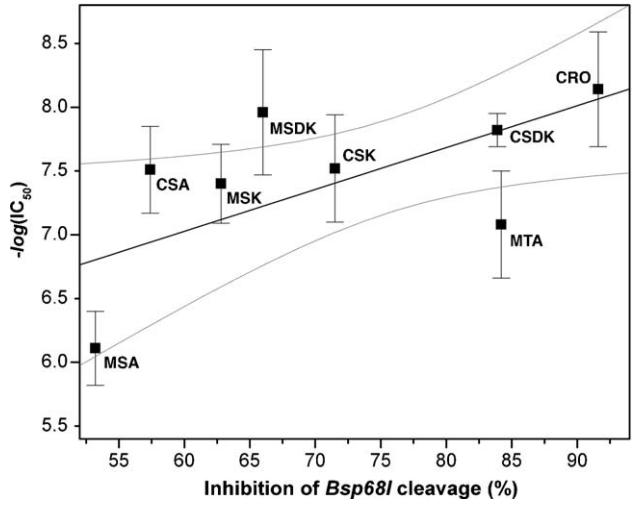

Fig. 6. Analysis of the correlation between the percentage of inhibition of *Bsp68I* cleavage by mithramycins and chromomycins and the average antiproliferative activity. Experimental data were fitted by weighted least-squares linear regression, in which the SD values were used as weight ($r = 0.741$, $p < 0.05$). Regions corresponding to the upper and lower 95% confidence limits are shown by gray lines.

In this context, we explored, with special emphasis on mithramycin analogues, other additional factors that may link the binding to DNA to an improved antiproliferative activity, such as their intracellular accumulation. The intracellular levels of several mithramycins and chromomycins were measured using two different human carcinoma cell lines (Fig. 7). After 4-h treatments, CRO was uptake better than MSDK, MSK and MTA by HCT116 colon cells. However, a time-course analysis of the intracellular levels up to 72 h revealed that while the levels of CRO decreased (which can indicate a certain efflux of the drug) those of MSDK increased to reach the higher concentration among the different molecules (Fig. 7A). The high uptake of MSDK by HCT116 cells was time-dependent up to 72 h in keeping with its outstanding biological activity (Fig. 5 and Table 1). After 72 hours incubation with the different drugs, the intracellular levels of the drugs were MSDK > MTA > MSK > CRO (Fig. 6A). In PC-3 human prostate cells, the uptake experiments revealed that, upon 48 h incubation, CRO was absorbed better than MSDK, MSK or MTA. Nevertheless, after 72 h, the MSDK intracellular levels remained higher than of the other antibiotics (Fig. 7B), in agreement with its superior antiproliferative activity.

4. Discussion

Drugs which interact with DNA so as to impair its function occupy a central place in cancer chemotherapy [37,38]. The formation of specific hydrogen bonds between the 8-O-hydroxyl group in MTA or CRO molecules and the 2-amino group of guanines plays a key role in their sequence-selective binding to G/C-rich DNA [13,22,24]. However, the role of the pentyl side chain linked to the C-3 of the chromophore has been barely characterized [17,20,23]. Therefore, we have analyzed six chromophore-modified molecules (Fig. 1) to gain further insights into the role of the long alkyl side chain in respect to DNA-binding preferences and antiproliferative activity.

Footprinting analyses have revealed that some subtle differences may exist between the binding of MTA or CRO to DNA [10,12,39]. Moreover, the analysis of the differences between MTA and MSK binding to DNA rendered almost indistinguishable footprints [20], which would suggest similar, if not the same, binding sites, while the analysis of their binding to heterogeneous DNA indicated a higher binding constant for MTA [23]. Further evidences on the preferred binding sites can be obtained from the protection of particular restriction enzyme cleavage sites by DNA-binding ligands [30,31,34,40]. We have examined the effects of eight mithramycins and chromomycins on *Eco52I*, *Bsp68I* and *AatII* restriction of linearized pBR322 plasmid DNA. In general, all the molecules inhibited cleavage by *Bsp68I* better than by *Eco52I* or *AatII*. Because the molecules assayed here are structurally related (Fig. 1), the differences in restriction enzyme cleavage in their presence should be directly linked to differences in sequence selectivity and DNA-binding affinity.

An effective drug design for the treatment of cancer requires not only 'disease specific' molecular targets, which would include DNA regulatory sequences, but reduced side-effects. Hence, we have

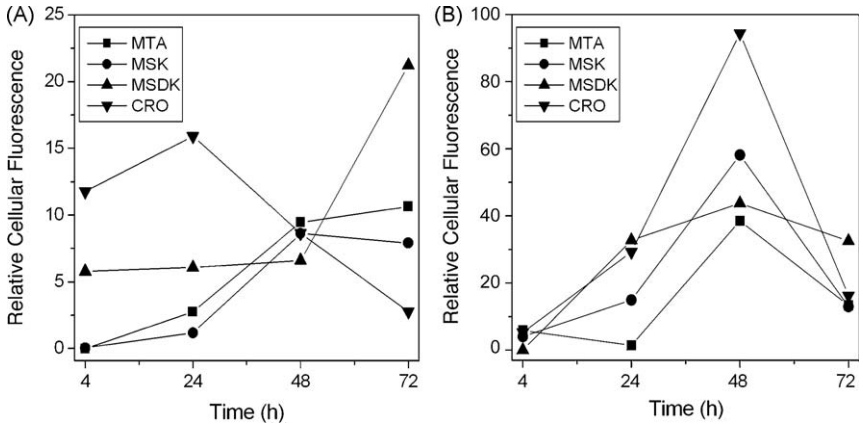

Fig. 7. Uptake and cellular retention of several mithramycins and chromomycins in human carcinoma cell lines. (A) Mean intracellular fluorescence measured from 1000 viable (propidium iodide-negative) HCT116 colon cells gated for analysis reveals time-course differences in both the uptake and retention of MTA, MSK, MSDK and CRO after incubation with 150 nM solutions of the different antibiotics for the times stated in the figure. (B) Mean intracellular fluorescence measured from 1000 viable (propidium iodide-negative) PC-3 prostate carcinoma cells gated for analysis reveals the time-course differences in both the uptake and retention of MTA, MSK, MSDK and CRO after incubation with 150 nM solutions of the different antibiotics for the times stated in the figure. Values represent mean from two independent experiments with similar results (±5%). Data in both panels correspond to aureolic acid antibiotics whose antiproliferative activity was measured in HCT116 or PC-3 (see Fig. 5).

explored the relationship that may exist between the capacity of mithramycins and chromomycins for inhibiting DNA cleavage by some restriction enzymes, which recognize different combinations of cytosines and guanines, the strength of binding to heterogeneous DNA, analyzed by the changes in DNA melting temperature, their uptake by cells, and the antiproliferative activity. A significant correlation was found between the protection from restriction cleavage by a variety of biosynthetically produced mithramycins and chromomycins and the changes they produced in DNA melting temperatures, in keeping with that both techniques would measure, albeit crude, how strong drug binding is. The restriction cleavage experiments and the changes in DNA melting temperature indicated that the "SK" and "SDK" analogues do not bind to DNA as tightly as the parental MTA or CRO. These results are consistent with that MTA has a higher DNA-binding constant than MSK [23].

NMR and footprinting analyses have indicated that MTA and CRO bind preferentially to DNA regions containing contiguous GC base pairs, although there are discrepancies on the exact composition of the binding sites [12,41]. Chromomycin can bind at GpC even though GpG is present, while the specificity of both MTA and CRO may extend over three bases within a larger binding site. The DNA-binding site of a Mg^{2+}-coordinated MTA or CRO dimers spans about five base pairs, which comprises the binding of their saccharide moieties along the minor groove of DNA [21,23,36]. Hence, the binding of the various chromophore-modified mithramycins and chromomycins to distinct C + G-rich sites might depend on the sequence environment in which the binding site is located. A DNAse I footprinting analysis using DNA fragments that contain every symmetrical hexanucleotide sequence, followed by a quantification of the degree of protection of the different binding sites, shows that MTA binds preferentially to AGCGCT over other sequences such as GGGCCC or TCGCGA [35]. These results are consistent with the preferred MTA binding site we have inferred from restriction enzyme cleavage, since the recognition site for *Bsp68I* contains the sequence TCGCGA, yet in the vicinity there are other C/G tracts (Fig. 2A) that may also represent alternative binding sites [21,35,39]. Closer inspection of the sequences flanking the unique *Eco52I* and *Bsp68I* restriction sites in pBR322 DNA (Fig. 2A) shows that the GpC step occurs three times at, or in the vicinity of, the restriction cleavage site. Moreover, previous footprinting assays presented evidence of binding of mithramycins to isolated C/G tracts, as those in the *AatII* restriction site, which was also partially protected, although to a different extent, by all the aureolic acid antibiotics (Fig. 4).

MSK and MSDK are more active than MTA against a variety of human cell lines (Fig. 5) in agreement with previously published data that suggested that these chromophore-modified analogues possess improved antiproliferative activity against some tumour cell lines [11,17,18], which is accompanied by an improved therapeutic index [11,17]. The data we have gathered on drug uptake and cellular retention of these molecules are in keeping with an improved biological profile that we evaluated through the comparison of their antiproliferative activities (Fig. 5).

Among the antibiotics studied here, MSA and CSA are those with lesser effect on ΔTm and restriction enzyme cleavage (Figs. 2–4), and MSA displays the weaker biological activity (Fig. 5 and Table 1). On the other hand, CRO and MTA bind tightly to DNA (Figs. 2–4 and Table 1), with CRO having also the higher antiproliferative activity (Table 1). MSDK may recognize some C/G-rich sequences better than MTA, such as some, if not all, putative binding sequences for the Sp1 transcription factor, thus altering the expression of various genes involved in cancer development [17]. It has been conjectured that MSK and MSDK may have a superior effect on Sp1-dependent promoters [17]. However, in the pursuit of therapies targeting transcription factors it is still unknown whether this improved molecular targeting by the chromophore-modified molecules is comparable to the effects of some bisanthracyclines on Sp1 binding to gene promoters [42].

In the present study, we have gained new insights into the DNA-binding properties and cytostatic/cytotoxic profiles of several chromophore-modified mithramycins and chromomycins. The utilization of the different analogues examined here, which can recognize different C/G-rich DNA sequences (Fig. 2) and attain different cytotoxic/cytostatic activities (Fig. 5) [17,18,43], might open new perspectives in cancer chemotherapy, as well as in the treatment of other pathologies, in which the parental MTA and CRO molecules have acquired renewed interest [6–9]. For CSK and CSDK the correlation between their structure (or more precisely their effects on restriction cleavage and DNA melting temperature) and function (measured as antiproliferative activity) was obvious (Table 1 and Fig. 6), while this was less evident for MSK and MSDK. Tentatively, the direct correlation between drug potency and DNA-binding specificity (Fig. 6), as well as differences in intracellular drug levels (Fig. 7), indicate that specific targeting rather than promiscuous poisoning give rise to potency that we have observed

among the chromophore-modified antibiotics It is worth noting that the activity of DNA-binding molecules, such of those analyzed here, would arise from the inhibition of RNA polymerases, which requires the efficient uptake of the drugs by the susceptible cells types.

Compared to MTA, MSK and MSDK bear shorter side chains attached at the three-position of the chromophore (Fig. 1). These shorter chains appear to make two effects in the chromophore-modified molecules. First, their binding to DNA is weaker, as substantiated by the inhibition of restriction cleavage and the smaller effect on DNA melting. Second, they show a higher antiproliferative effect. The cause of this improved activity, which is more evident in some cell types (Fig. 5 and [17,18]), can be a higher intracellular retention of the molecules bearing shorter alkyl chains by cells (Fig. 7 and [17]), but also of some peculiarities in the mechanisms of cell death triggered by these drugs [18]. An equivalent reasoning can be used when considering the different chromomycin analogues. Nonetheless, when comparing to MTA, the results obtained with chromophore-modified chromomycins should be handled with caution because CRO endures both a worse therapeutic index [44] and a higher toxicity in animal models [45]. Whether the fast uptake of CRO observed in two different cell types (Fig. 7) might be related to a more ''indiscriminate'' toxicity in cells cannot be defined from the present results, although the behaviour of CRO was clearly different from that of MTA which bears the some chromophore. The chromophore-modified chromomycins could incorporate some of the potential disadvantages of CRO [44]. Despite this, the development of chromophore-modified chromomycins is still of interest [25], especially because such molecules may be useful in the treatment of some peculiar pathologies [8].

In summary, the results presented in this paper support the usefulness of studying the protection of restriction sites from cleavage as a method to explore the specificity of DNA–ligand interactions. They established the sequence-selective binding of the different aureolic acid antibiotics within or in the vicinity of some restriction sites. Besides, we have observed a fair correlation between the antiproliferative activities of the different chromophore-modified mithramycins and chromomycins and their improved binding to certain C/G-rich restriction sites. This correlation, while being mathematically precise, is a simplification of the real situation, and thus we have explored other molecular events occurring within cells that may explain the cytotoxicity and promising biological activity of these molecules, fundamentally MSK and MSDK. The differences observed in the uptake and retention of aureolic acid antibiotics by some cell types was useful to explain the improved antiproliferative activities observed for some of the analogues.

Acknowledgements

We are thankful to Ms. Leire Neri, Ms. Malgorzata Kwaśniak and Dr. Marc Bataller for helping us in some of the experiments. This work was supported by grants from the former Spanish Ministry of Education and Science (BFU2007-60998) and the FEDER program of the European Community (to JP), and from ''Red Temática de Investigación Cooperativa de Centros de Cáncer'' (Ministry of Health, Spain; ISCIII-RETIC RD06/0020/0026) (to JAS). It has been carried out within the framework of the 'Xarxa de Referencia en Biotecnologia' of the Generalitat de Catalunya.

Appendix A. Supplementary data

Supplementary data associated with this article can be found, in the online version, at doi:10.1016/j.bcp.2010.01.005.

References

[1] Lombó F, Menéndez N, Salas JA, Méndez C. The aureolic acid family of antitumor compounds: structure, mode of action, biosynthesis, and novel derivatives. Appl Microbiol Biotechnol 2006;73:1–14.
[2] Wohlert SE, Kunzel E, Machinek R, Méndez C, Salas JA, Rohr J. The structure of mithramycin reinvestigated. J Nat Prod 1999;62:119–21.
[3] DeVita VTJ, Hellman S, Rosenberg SA. Cancer: principles & practice of oncology. Philadelphia, PA: Lippincott Williams & Wilkins; 2005.
[4] Ogawa M. A recent overview of chemotherapy for advanced stomach cancer in Japan. Antibiot Chemother 1978;24:149–59.
[5] Bianchi N, Osti F, Rutigliano C, Corradini FG, Borsetti E, Tomassetti M, et al. The DNA-binding drugs mithramycin and chromomycin are powerful inducers of erythroid differentiation of human K562 cells. Br J Haematol 1999;104:258–65.
[6] Ferrante RJ, Ryu H, Kubilus JK, D'Mello S, Sugars KL, Lee J, et al. Chemotherapy for the brain: the antitumor antibiotic mithramycin prolongs survival in a mouse model of Huntington's disease. J Neurosci 2004;24:10335–42.
[7] Fibach E, Bianchi N, Borgatti M, Prus E, Gambari R. Mithramycin induces fetal hemoglobin production in normal and thalassemic human erythroid precursor cells. Blood 2003;102:1276–81.
[8] Sutphin PD, Chan DA, Li JM, Turcotte S, Krieg AJ, Giaccia AJ. Targeting the loss of the von Hippel-Lindau tumor suppressor gene in renal cell carcinoma cells. Cancer Res 2007;67:5896–905.
[9] Jia Z, Zhang J, Wei D, Wang L, Yuan P, Le X, et al. Molecular basis of the synergistic antiangiogenic activity of bevacizumab and mithramycin A. Cancer Res 2007;67:4878–85.
[10] Fox KR, Howarth NR. Investigations into the sequence-selective binding of mithramycin and related ligands to DNA. Nucleic Acids Res 1985;13:8695–714.
[11] Remsing LL, González AM, Nur-e-Alam M, Fernández-Lozano MJ, Braña AF, Rix U, et al. Mithramycin SK, A novel antitumor drug with improved therapeutic index, mithramycin SA, and demycarosyl-mithramycin SK: three new products generated in the mithramycin producer *Streptomyces argillaceus* through combinatorial biosynthesis. J Am Chem Soc 2003;125:5745–53.
[12] Van Dyke MW, Dervan PB. Chromomycin, mithramycin, and olivomycin binding sites on heterogeneous deoxyribonucleic acid. Footprinting with (methidiumpropyl-EDTA)iron(II). Biochemistry 1983;22:2373–7.
[13] Gao XL, Mirau P, Patel DJ. Structure refinement of the chromomycin dimer–DNA oligomer complex in solution. J Mol Biol 1992;223:259–79.
[14] Sastry M, Patel DJ. Solution structure of the mithramycin dimer–DNA complex. Biochemistry 1993;32:6588–604.
[15] Aich P, Dasgupta D. Role of magnesium ion in mithramycin–DNA interaction: binding of mithramycin–Mg^{2+} complexes with DNA. Biochemistry 1995;34:1376–85.
[16] Aich P, Sen R, Dasgupta D. Role of magnesium ion in the interaction between chromomycin A_3 and DNA: binding of chromomycin A_3–Mg^{2+} complexes with DNA. Biochemistry 1992;31:2988–97.
[17] Albertini V, Jain A, Vignati S, Napoli S, Rinaldi A, Kwee I, et al. Novel G/C-rich DNA-binding compound produced by a genetically engineered mutant of the mithramycin producer *Streptomyces argillaceus* exhibits improved transcriptional repressor activity: implications for cancer therapy. Nucleic Acids Res 2006;34:1721–34.
[18] Bataller M, Méndez C, Salas JA, Portugal J. Mithramycin SK modulates polyploidy and cell death in colon carcinoma cells. Mol Cancer Ther 2008;7:2988–97.
[19] Blume SW, Snyder RC, Ray R, Thomas S, Koller CA, Miller DM. Mithramycin inhibits Sp1 binding and selectively inhibits transcriptional activity of the dihydrofolate reductase gene in vitro and in vivo. J Clin Invest 1991;88:1613–21.
[20] Remsing LL, Bahadori HR, Carbone GM, McGuffie EM, Catapano CV, Rohr J. Inhibition of *c-src* transcription by mithramycin: structure–activity relationships of biosynthetically produced mithramycin analogues using the *c-src* promoter as target. Biochemistry 2003;42:8313–24.
[21] Keniry MA, Banville DL, Simmonds PM, Shafer R. Nuclear magnetic resonance comparison of the binding sites of mithramycin and chromomycin on the self-complementary oligonucleotide $d(ACCCGGGT)_2$. Evidence that the saccharide chains have a role in sequence specificity. J Mol Biol 1993;231:753–67.
[22] Hou MH, Robinson H, Gao YG, Wang AH. Crystal structure of the [Mg^{2+}–(chromomycin $A_3)_2$]–$d(TTGGCCAA)_2$ complex reveals GGCC binding specificity of the drug dimer chelated by a metal ion. Nucleic Acids Res 2004;32:2214–22.
[23] Barceló F, Scotta C, Ortiz-Lombardía M, Méndez C, Salas JA, Portugal J. Entropically-driven binding of mithramycin in the minor groove of C/G-rich DNA sequences. Nucleic Acids Res 2007;35:2215–26.
[24] Sastry M, Fiala R, Patel DJ. Solution structure of mithramycin dimers bound to partially overlapping sites on DNA. J Mol Biol 1995;251:674–89.
[25] Menéndez N, Nur-e-Alam M, Braña AF, Rohr J, Salas JA, Méndez C. Biosynthesis of the antitumor chromomycin A_3 in *Streptomyces griseus*: analysis of the gene cluster and rational design of novel chromomycin analogs. Chem Biol 2004;11:21–32.
[26] Rodríguez D, Quirós LM, Salas JA. MtmMII-mediated C-methylation during biosynthesis of the antitumor drug mithramycin is essential for biological activity and DNA–drug interaction. J Biol Chem 2004;279:8149–58.
[27] Blanco G, Fernández E, Fernández MJ, Braña AF, Weissbach U, Kunzel E, et al. Characterization of two glycosyltransferases involved in early glycosylation

steps during biosynthesis of the antitumor polyketide mithramycin by *Streptomyces argillaceus*. Mol Gen Genet 2000;262:991–1000.
[28] Rohr J, Méndez C, Salas JA. The biosynthesis of aureolic group antibiotics. Bioorg Chem 1999;27:41–54.
[29] Baig I, Perez M, Braña AF, Gomathinayagam R, Damodaran C, Salas JA, et al. Mithramycin analogues generated by combinatorial biosynthesis show improved bioactivity. J Nat Prod 2008;71:199–207.
[30] Malcolm AD, Moffatt JR. Differential reactivities at restriction enzyme sites. Biochim Biophys Acta 1981;655:128–35.
[31] Párraga A, Portugal J. Detection of elsamicin–DNA binding specificity by restriction enzyme cleavage. FEBS Lett 1992;300:25–9.
[32] Wilson WD, Tanious FA, Fernandez-Saiz M, Rigl CT. Evaluation of drug–nucleic acid interactions by thermal melting curves. Methods Mol Biol 1997;90:219–40.
[33] Mosmann T. Rapid colorimetric assay for cellular growth and survival: application to proliferation and cytotoxicity assays. J Immunol Methods 1983;65:55–63.
[34] Chaires JB, Fox KR, Herrera JE, Britt M, Waring MJ. Site and sequence specificity of the daunomycin–DNA interaction. Biochemistry 1987;26:8227–36.
[35] Hampshire AJ, Fox KR. The effects of local DNA sequence on the interaction of ligands with their preferred binding sites. Biochimie 2008;90:988–98.
[36] Majee S, Sen R, Guha S, Bhattacharyya D, Dasgupta D. Differential interactions of the Mg^{2+} complexes of chromomycin A_3 and mithramycin with Poly(dG-dC)·Poly(dC-dG) and Poly(dG)·Poly(dC). Biochemistry 1997;36:2291–9.
[37] Hurley LH. DNA and its associated processes as targets for cancer therapy. Nat Rev Cancer 2002;2:188–200.
[38] Portugal J. Evaluation of molecular descriptors for antitumor drugs with respect to noncovalent binding to DNA and antiproliferative activity. BMC Pharmacol 2009;9:11.
[39] Stankus A, Goodisman J, Dabrowiak JC. Quantitative footprinting analysis of the chromomycin A_3–DNA interaction. Biochemistry 1992;31:9310–8.
[40] Malcolm AD, Moffatt JR, Fox KR, Waring MJ. Differential inhibition of a restriction enzyme by quinoxaline antibiotics. Biochim Biophys Acta 1982;699:211–6.
[41] Cons BM, Fox KR. High resolution hydroxyl radical footprinting of the binding of mithramycin and related antibiotics to DNA. Nucleic Acids Res 1989;17:5447–59.
[42] Mansilla S, Portugal J. Sp1 transcription factor as a target for anthracyclines: effects on gene transcription. Biochimie 2008;90:976–87.
[43] Bataller M, Méndez C, Salas JA, Portugal J. Cellular response and activation of apoptosis by mithramycin SK in $p21^{WAF1}$-deficient HCT116 human colon carcinoma cells. Cancer Lett; in press. doi:10.1016/j.canlet.2009.11.008.
[44] Slavik M, Carter SK. Chromomycin A_3, mithramycin, and olivomycin: antitumor antibiotics of related structure. Adv Pharmacol Chemother 1975;12:1–30.
[45] Singh B, Gupta RS. Species-specific differences in the toxicity and mutagenicity of the anticancer drugs mithramycin, chromomycin A_3, and olivomycin. Cancer Res 1985;45:2813–20.